Built Environments, Inc.
www.built-environments.com

MOISTURE PERFORMANCE REPORT

Report No.: 012019-2

Issued to:

QUIK-THERM SOLUTIONS, INC.

1680 Sargent Ave. Unit 3
Winnipeg, MB
Canada, R3H 0C2

ASSEMBLY: Solar Dry Insulation on Wood Framed Construction

Issued by:

Built Environments, Inc.
2850 Curve Crest Blvd. W. Suite 220
Stillwater, Minnesota 55082

Phone: 651.439.9396
Fax: 651.204.2247

1.0 Executive Summary

This study evaluated moisture performance of a wood-framed wall assembly configured with the Quik-Therm Solar Dry Insulation system. This system employs expanded polystyrene (EPS) panels with perforated, vapor-permeable metalized polymer facers. The insulation panels are uniquely configured with recessed profiles that form vertical drainage voids on either side of the panel. The front side offers a ventilated rainscreen space while the back side creates a series of pressure-equalized chambers when constructed with upper termination closures and taped panel joints.

Study Design

Analyses were performed in three phases. The first phase assessed transient moisture transport through a one-dimensional wall assembly. Hygrothermal simulations were performed for three climates: Vancouver, British Columbia; Winnipeg, Manitoba; and Toronto, Ontario. All three modeled climates indicated peak moisture levels associated with the coldest months of each year.

The second phase of study evaluated steady-state moisture transport in a two-dimensional wall. This assembly was analyzed in section view for a 10-foot (3 m) wall height. The purpose of this approach was to evaluate moisture performance during winter design conditions. Two-dimensional modeling was also used to describe airflow characteristics within the intended drainage space.

The final phase of study assessed steady-state moisture transport in a three-dimensional wall assembly. These analyses also assessed moisture performance during winter design conditions.

Results

Transient one-dimensional analyses revealed higher moisture levels associated with Year 0 through the first cold season of Year 1. This initial moisture burden was attributed to construction moisture as simulated by an initial relative humidity of 80% across all wall components. Subsequent peaks in moisture levels were associated with winter conditions and episodic wind-driven rain events during wet seasons. In all instances, moisture levels were maintained below critical thresholds associated with mold growth and material degradation. Furthermore, simulation outcomes showed no evidence of consecutive moisture accumulation during the 10-year simulation periods. The predicted outcomes for Years 0-3 are provided in Section 6 of this report.

Steady-state analyses demonstrated effective vapor transport through the panel's perforated facers and vapor-open drainage space. Moisture accumulation within the assembly was not observed. The bottom termination of the drainage space provided an open boundary where air was free to flow bi-directionally under the constraints of natural convection. Airflows were characterized by laminar flow, low airflow velocities, and limited air exchange with the adjacent exterior air. These conditions provided the required provisions for free drainage without compromise to thermal efficiency.

Conclusions

1.1 Moisture levels during Year 0 through the first cold season of Year 1 were attributed to construction moisture, which was simulated as 80% relative humidity across all assembly layers. Corresponding surface temperatures during these periods were sufficiently low to reduce the risks of mold and degradation below recognized evaluation criteria (ASHRAE 160, Addendum E). Likewise, hygric conditions for the full 10-year simulation periods were within acceptable limits for all test climates.

1.2 Simulations employed a 6-mil polyethylene membrane as an interior vapor barrier. Initial analyses showed similar results with 'smart' vapor retarders that exhibit moisture-dependent vapor permeance. Likewise, interior vapor barrier paints (<0.5 perms) may be used in lieu of the polyethylene vapor barrier. These alternate approaches may improve performance during hot, humid conditions.

1.3 Moisture performance was largely determined by vapor diffusion through the insulation panel's perforated facers. The assumed perforated area was 1%, which corresponds to a thin moisture barrier with a water vapor permeance of approximately 11 U.S. Perms. This is an order of magnitude higher than the un-faced EPS insulation panel.

1.4 Drainage spaces were modeled as full-wall height voids with closures at the upper terminations. These closures prevented non-circulating airflows and associated thermal bypasses behind the insulation panel. The upper closures, together with the flush-mounted stud interfaces, represent partially closed chambers that are essentially pressure equalized under forced convection (e.g. wind).

1.5 The drainage closures were simulated as closed cell spray foam, which accommodated vapor release while remaining impermeable to airflow at encountered pressures. It is important to note that performance does not rely on vapor release at the top termination. Actual construction may therefore consider vapor-impermeable closures that offer similar air-tight performance.

1.6 Simulations did not consider imperfections such as insulation gaps. Actual in-service performance assumes air-tight seals at all gaps and thru-wall penetrations. Furthermore, fastener penetrations are not expected to alter moisture performance as fasteners through the EPS insulation are reasonably self-sealing. Penetrations through the water-resistive barrier were considered by hygrothermal analyses where a 1% wind-driven rain load was distributed throughout the entire WRB layer.

1.7 Natural convection within the open drainage channels did not significantly affect moisture or thermal performance. While the open channels enhanced vapor release, diffusion occurred primarily through the perforated insulation system. Airflow velocities and resulting air changes within the drainage space were a function of temperature gradients across the wall. At large temperature differences (e.g. -10°F exterior; 70°F interior), average airflow velocities were only 0.00058 m/s. This corresponds to 0.34 air changes per hour when assuming 100% air exchange with the adjacent exterior air layer. The predicted reduction in thermal efficiency was less than 1%.

2.0 Assembly: One-Dimensional Assembly (Transient Moisture Transport)

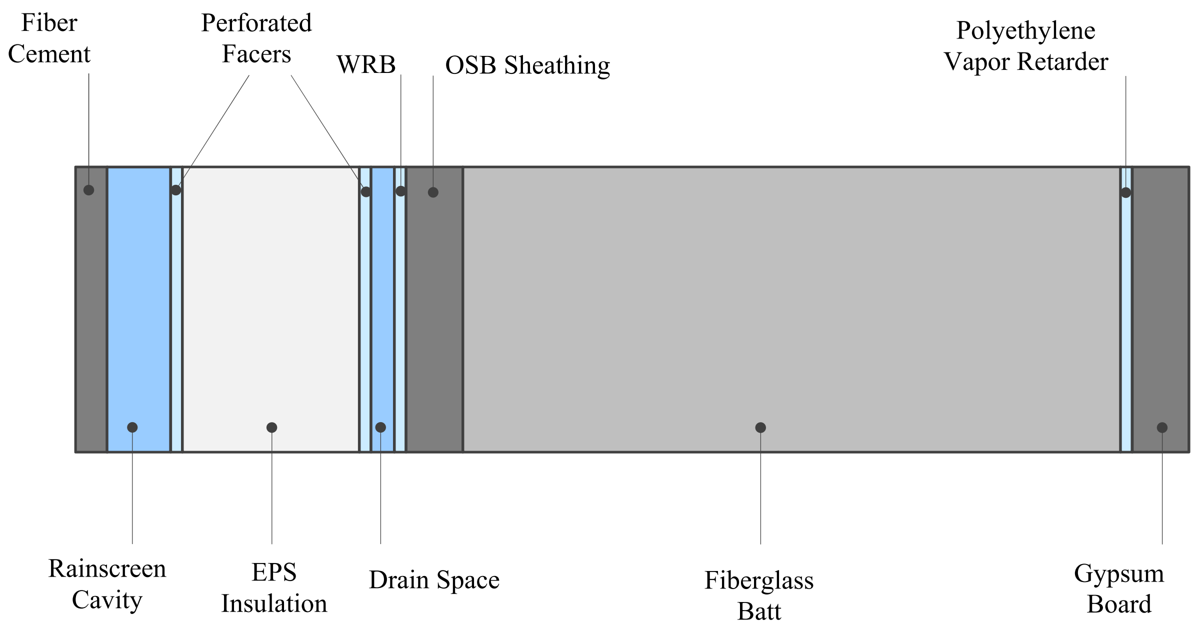

1	Fiber Cement Siding: 0.3125 in. (7.94 mm)*
2	Ventilated Rainscreen Cavity: 0.5625 in. (14.3 mm); ventilated at 10 ACH
3	Perforated Metalized Polymer Facer
4	Expanded Polystyrene Insulation: 1.5 in. (38.1 mm)
5	Perforated Metalized Polymer Facer
6	Drain Space: 0.1875 in. (4.76 mm)
7	Water-Resistive Barrier (50 perms)
8	Oriented Strand Board - OSB: 0.5 in. (12.7 mm)
9	Low Density Fiberglass Insulation: 5.5 in. (139.7 mm)
10	Polyethylene Vapor Retarder (6-mil)
11	Interior Gypsum Board: 0.5 in (12.7 mm)

* stated layer thicknesses remained consistent for the two- and three-dimensional assemblies (see Section 2.1)

2.1 Assembly: Two- and Three-Dimensional Assemblies (Steady-State Moisture Transport)

Isometric View

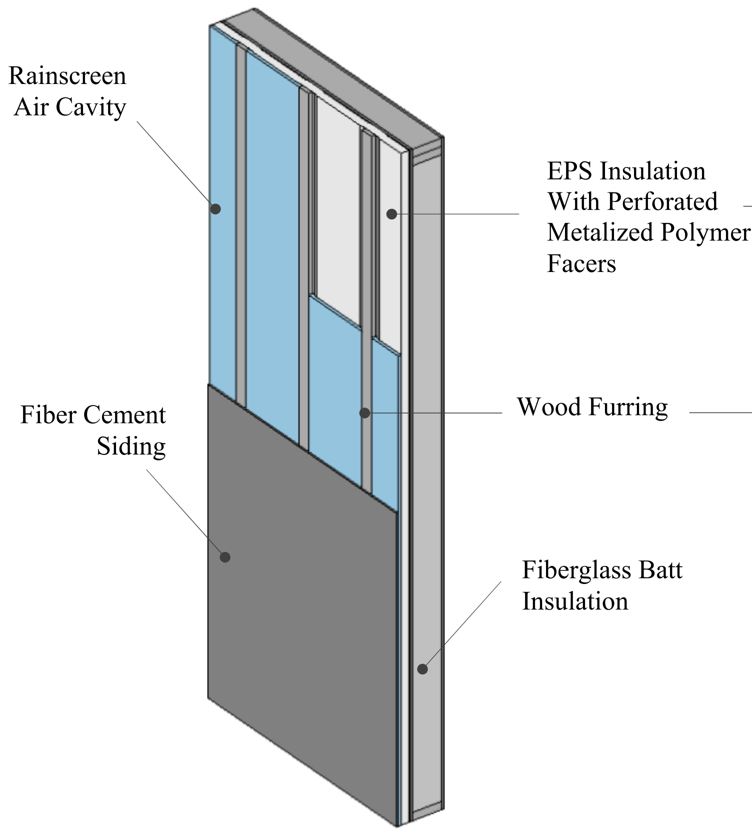

Plan View (top plate omitted)

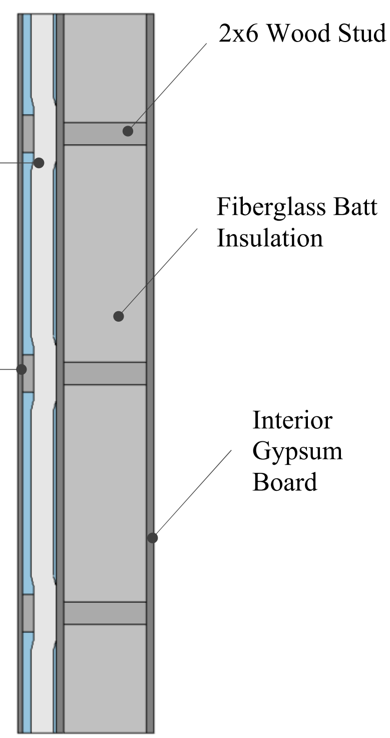

Section View: Top

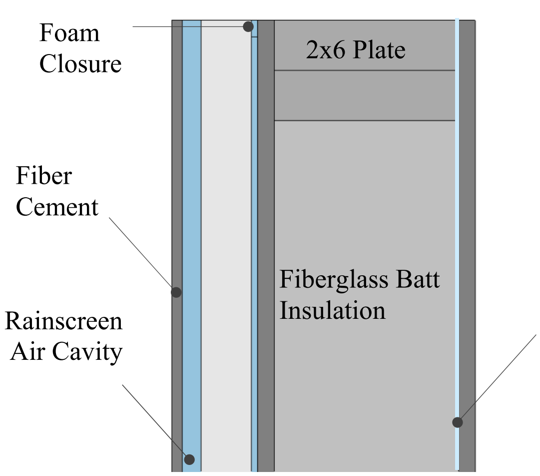

Section View: Top

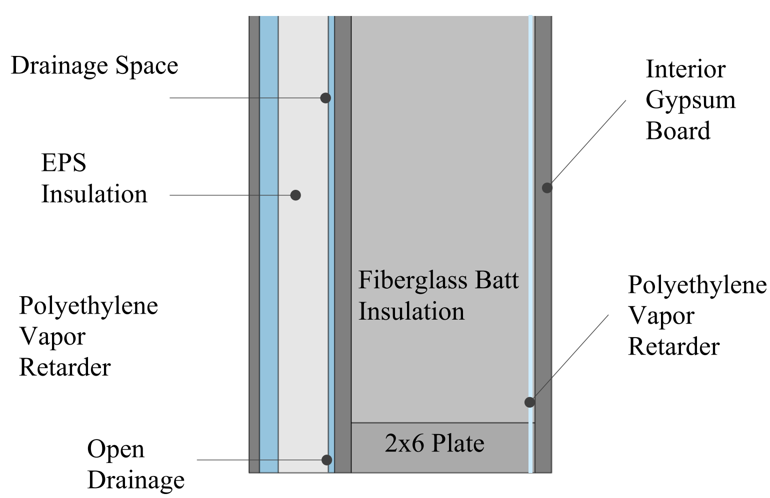

3.0 Methods: Transient Moisture

This assessment employed WUFI® Pro 6.2 hygrothermal modeling software developed jointly by the Oak Ridge National Laboratory (ORNL) and Germany's Fraunhofer Institute of Bauphysics (IBP). This software is designed to model transient, one-dimensional movement of heat and moisture through building assemblies.

Unless otherwise stipulated, simulations were performed in accordance with design parameters outlined by ASHRAE 160-2009, *Criteria for Moisture-Control Design Analysis in Buildings* and Addendum E. Preliminary analyses accounted for typical model variations such as building orientation, climate data sets, interior climate conditions, and surface transfer coefficients. Initial simulations reflected a ten-year period with calculation start and end dates of October 1 and December 31, respectively. The reported findings reflect Years 0-3. Final model assumptions are stipulated below (Tables 3.1 and 3.2).

Interior design conditions were determined by WUFI's integrated EN 15026 / WTA 6-2 interior climate method. The variation of the indoor air temperature is derived from the outdoor air temperature via a specified transfer function. The 'Normal Case' pre-defined transfer function was employed in these analyses: Medium Moisture Load: residential spaces and similar rooms, including kitchens and bathrooms.

Exterior weather data utilized WUFI's Cold Year meteorological data for 1) Vancouver, British Columbia, 2) Winnipeg, Manitoba; and 3) Toronto, Ontario.

Model assumptions for building exposure, air & moisture sources, and surface transfer coefficients are summarized in Tables 3.1 and 3.2.

Table 3.1. Exposure & Air/Moisture Sources

Parameter	Value / Condition
Orientation	North
Inclination	90°
Rain Exposure Factor	1.0
Building Height	<10 m
Exposure Category	Medium
Rain Deposition Factor	0.35
Rainscreen Air Change	10 ACH
Moisture Source	1% Driving Rain*
Moisture Clipping	Free Water Saturation
Air Infiltration Model	Class B (3 m^3/m^2h)
Stack Height	5 m
Moisture Clipping	Free Water Saturation

* ASHRAE 160 (applied to exterior surface of WRB)

Table 3.2. Surface Coefficients & Initial Conditions

Parameter	Value
Exterior Surface: Heat Transfer	Wind-Dependent
Exterior Permeance	sd value = 0.5 m
Short-Wave Radiation Absorptivity	0.5
Long-Wave Radiation Emissivity	-
Explicit Radiation Balance	-
Ground Short-Wave Reflectivity	0.2
Adhering Fraction of Rain	0.7
Interior Surface: Heat Transfer	8.0 W/m^2K
Interior Permeance	sd value = 0.5 m
Initial Condition: RH	80%
Initial Condition: Temperature	20°C (68°F)

Performance Criteria and Risk Evaluation

Simulation outcomes were compared to the VTT Mold Index evaluation criteria as outlined in ASHRAE 160 (2009), Addendum E.   The Mold Index was determined using the WUFI-integrated Mold Index VTT plug-in.

The VTT Mold Model is an empirical model based on the visual findings of mold growth coverage on material surfaces. The level of mold growth is represented by six index values, where level 1 corresponds to the first microscopic signs of mold and level 6 corresponds to total coverage of mold. The mold index is derived from: 1) the predicted temperature and humidity conditions; 2) the material sensitivity class; and 3) the surface location within the assembly.

Table 3.3. VTT Mold Index

Value	Description
0	No growth
1	Small amounts of mold on surface, initial stages of local growth
2	Several local mold growth colonies on surface
3	Visual findings of mold on surface, < 10% coverage, or, < 50% coverage of mold
4	Visual findings of mold on surface, 10 − 50% coverage, or, > 50% coverage of mold
5	Plenty of growth on surface, > 50% coverage (visual – without microscopic aid)
6	Heavy and tight growth, coverage about 100% (visual – without microscopic aid)

Exterior and interior surfaces of wall sheathing were selected as reference surfaces for assessment of potential moisture accumulation and associated risks.   Moisture risks were assessed on the basis of mold growth and degradation as described above for the VTT Mold Index Model.

The sensitivity class assumed by these analyses was ‘Sensitive’, Pine Sapwood. The relative coefficient for mold index decline was 0.25 as recommended for conservative estimates for mold growth.

Table 3.4. Evaluation Criteria

Mold Index	Description
<1	Acceptable, **low risk** of mold growth and degradation
>1 to 3	Borderline, **possible risk** of mold growth and degradation
>3	Unacceptable, **high risk** of mold growth and degradation

4.0 Methods: Steady-State Moisture Transport

This assessment applied Computational Fluid Dynamics to simulate coupled heat and moisture transport through two- and three-dimensional wall assemblies. Simulations were performed using COMSOL Multiphysics 5.4, which employs partial differential equations and Finite Element Analysis (FEM) to predict simultaneous flows of fluids, gasses, heat, and moisture. CFD simulations were performed in accordance with best practice guidelines and the COMSOL Multiphysics user's guide for version 5.4.

Unlike dew point analysis, which evaluates the likelihood of condensation based on one-dimensional, steady-state temperature profiles, CFD analysis utilizes three-dimensional vapor diffusion modeling. Vapor permeability, water contents, and diffusion characteristics for each assembly component are therefore considered. Steady-state analysis of vapor diffusion and the likelihood of moisture accumulation were evaluated based on temperature and moisture gradients as established from both sides of the wall assembly. Simulations assumed the following steady-state conditions:

Table 4.1. Assumed Conditions and Transfer Coefficients

Condition	Heat Flux	Moisture Flux
Temperature: Interior	70°F (21.1°C)	70°F (21.1°C)
Temperature: Exterior	-10°F (-23.2°C)	-10°F (-23.2°C)
Relative Humidity: Interior	-	40%
Relative Humidity: Exterior	-	80%
Heat Transfer Coefficients	Interior: 8.0 W/m^2K Exterior: 17 W/m^2K	-
Moisture Transfer Coefficients	-	Interior: 8.0^{-8} s/m Exterior: 25^{-8} s/m

CFD simulations evaluated coupled heat and moisture transfer through a typical area of the wall assembly as described in Section 2.1. Wall dimensions were 4 ft (1.2 m) wide by 10 ft (3 m) high. The upper termination of the drainage space behind the Solar Dry Insulation panel contained a 0.5-inch (12.7 mm) closure. For the purpose of this analysis, the closure consisted of closed cell polyurethane foam. The intent of the closure was to prevent non-circulating circulation within the drainage space. Initial analyses employing 'fluid air' within a two-dimensional drainage space are reported in Section 6.3. These results indicated no appreciable affects associated with fluid flows. The final three-dimensional analyses simulated the drainage space as 'solid air', which assumed effective material properties consistent with a solid 5 mm air layer (see Material Properties – Section 5.0).

5.0 Material Properties

Component	Vapor Resistance Factor	Density lb/ft^3 (kg/m^3)	Heat Capacity BTU/lb°F (J/kg-K)	Conductivity BTU in/hr ft^2°F (W/mK)
Wood Furring (Spruce)	552	25.0 (400)	0.449 (1,880)	0.597 (0.086)
Expanded Polystyrene	73	0.92 (14.8)	0.351 (1,470)	0.250 (0.036)
Top Plates (Spruce)	552	25.0 (400)	0.449 (1,880)	0.597 (0.086)
Bottom Plate (Spruce)	552	25.0 (400)	0.449 (1,880)	0.597 (0.086)
Wood Framing (Spruce)	552	25.0 (400)	0.449 (1,880)	0.597 (0.086)
Oriented Strand Board	812	40.6 (650)	0.449 (1,880)	0.638 (0.092)
Low Density Fiberglass Batt	1.2	0.55 (8.8)	0.201 (840)	0.286 (0.0412)
Interior Gypsum Board	7.0	53.1 (850)	0.208 (870)	1.11 (0.16)
Air/Drainage Space	0.79	0.081 (1.3)	0.239 (1,000)	0.326 (0.047)
Closed Cell Polyurethane Foam	89	2.43 (39)	0.351 (1,470)	0.173 (0.025)
Rainscreen Air Cavity	0.56	0.081 (1.3)	0.238 (1,000)	0.902 (0.13)
Fiber Cement Siding	990.9	86.1 (1,380)	0.20 (840)	1.70 (0.245)

6.0 Results: Transient Moisture - Vancouver, British Columbia

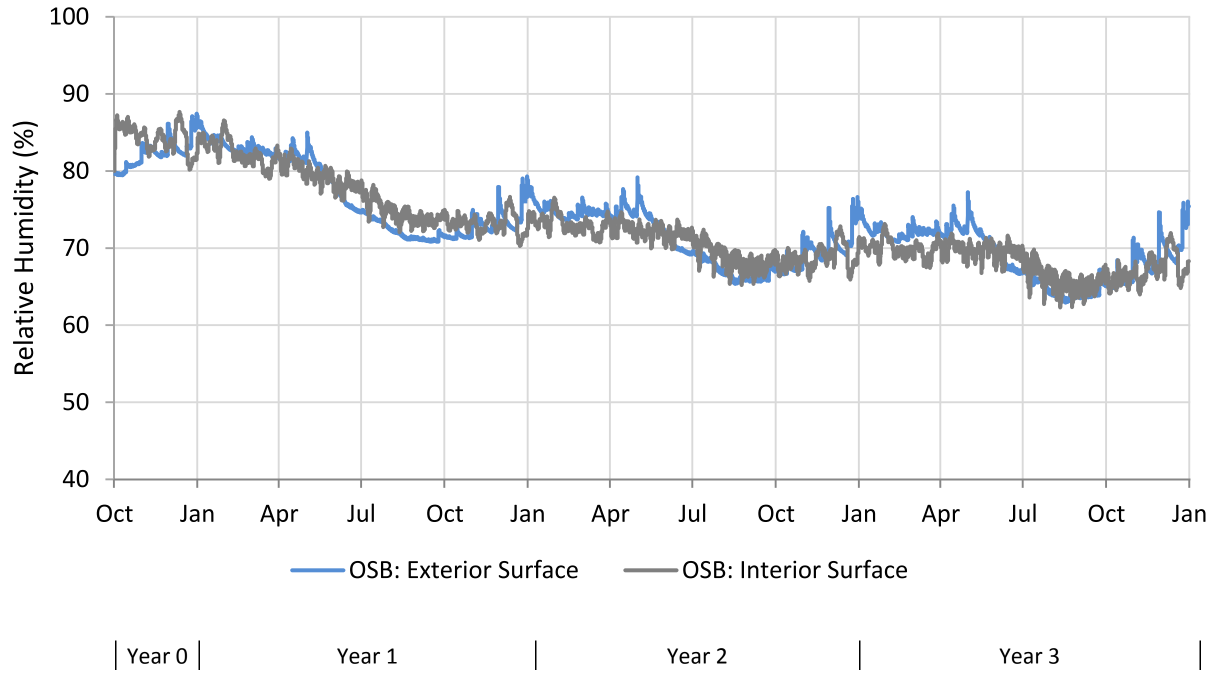

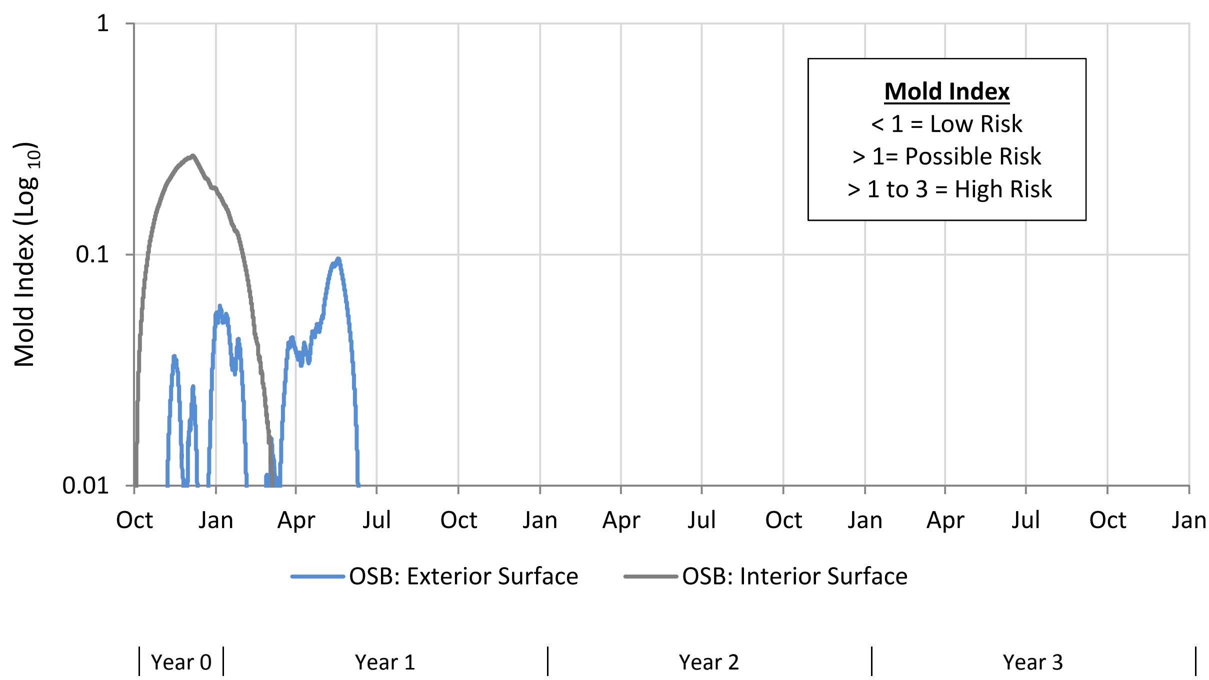

6.1 Results: Transient Moisture - Winnipeg, Manitoba

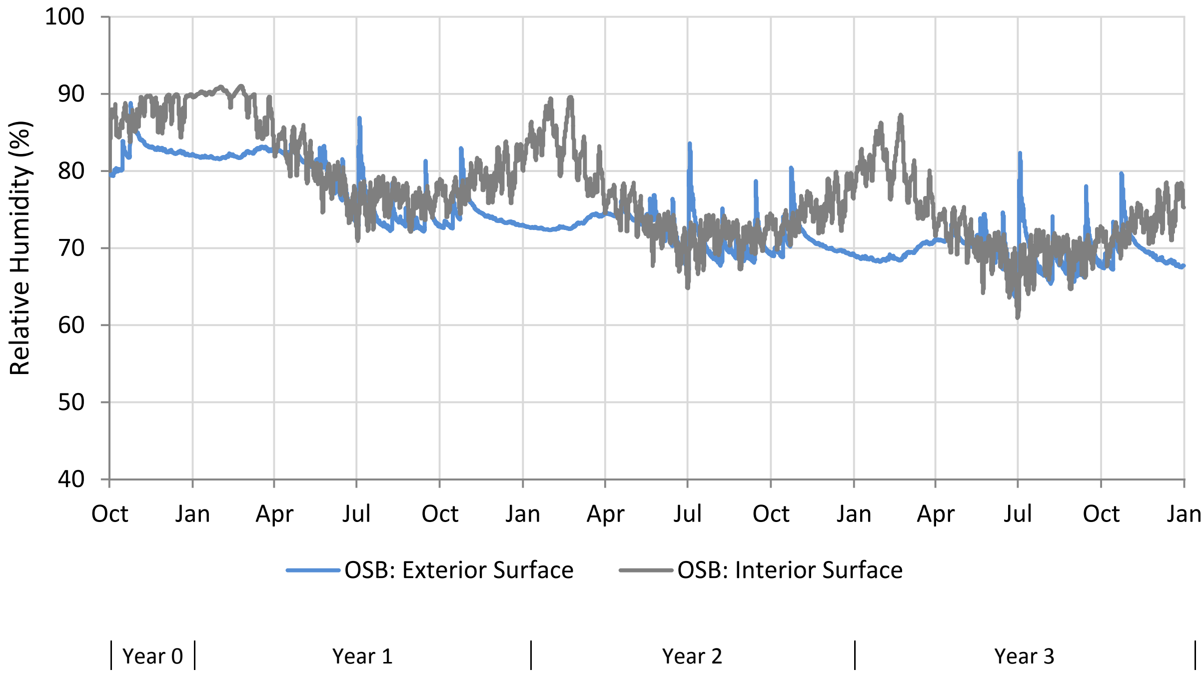

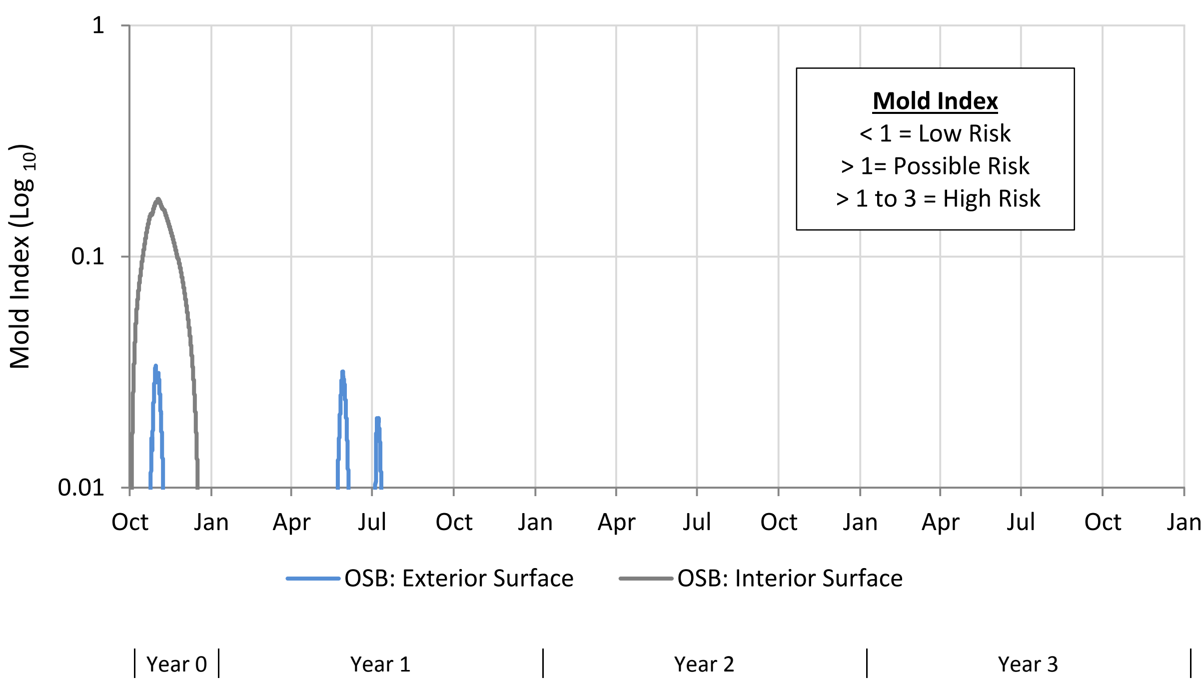

6.2 Results: Transient Moisture - Toronto, Ontario

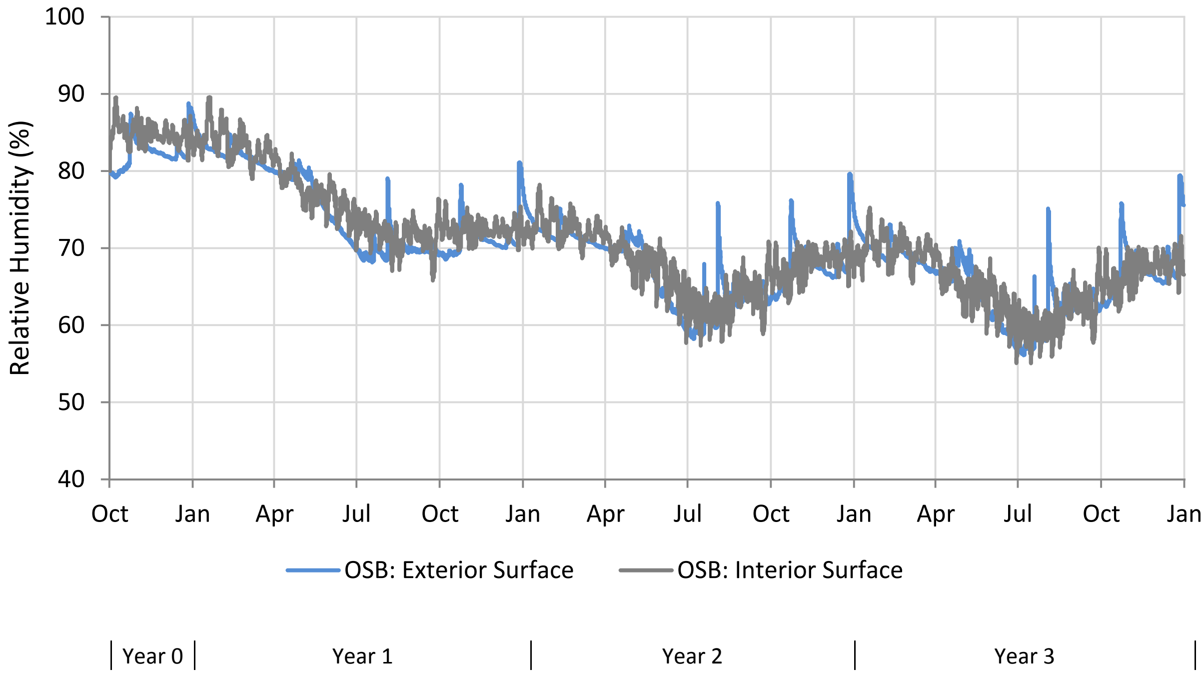

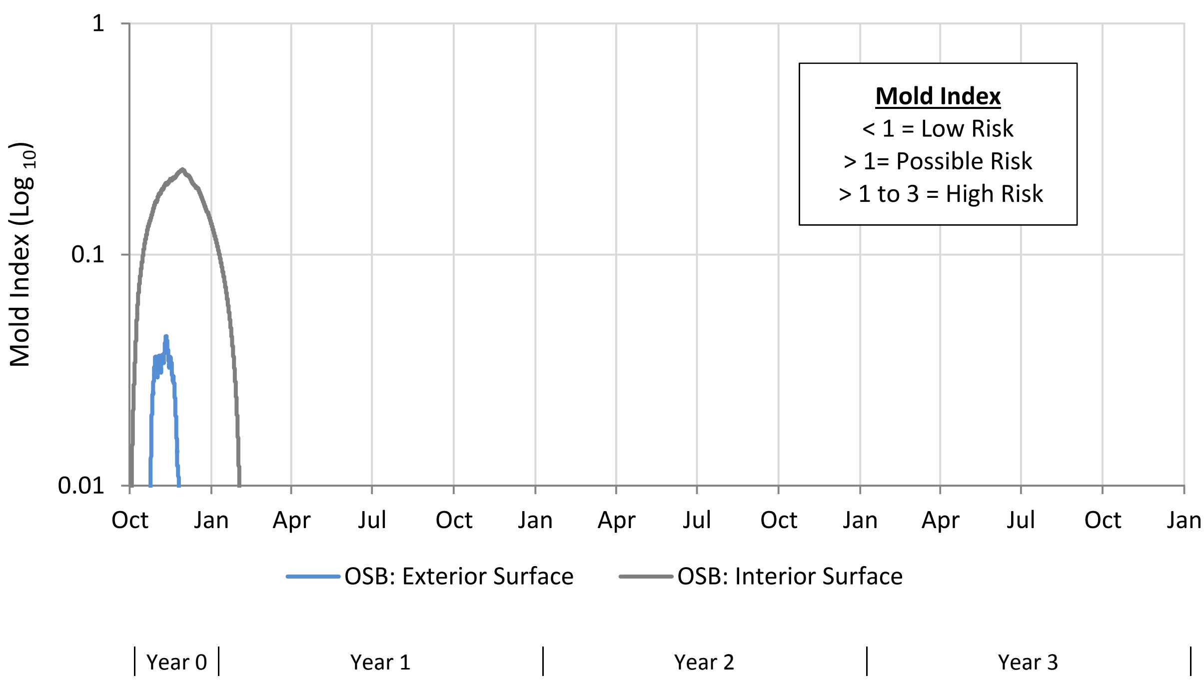

6.3 Results: Two-Dimensional Airflow (Drainage Space Airflow)

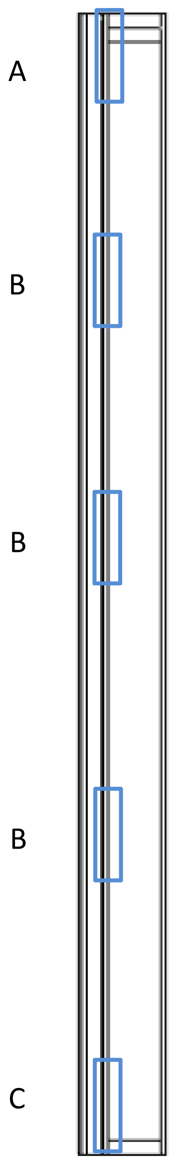

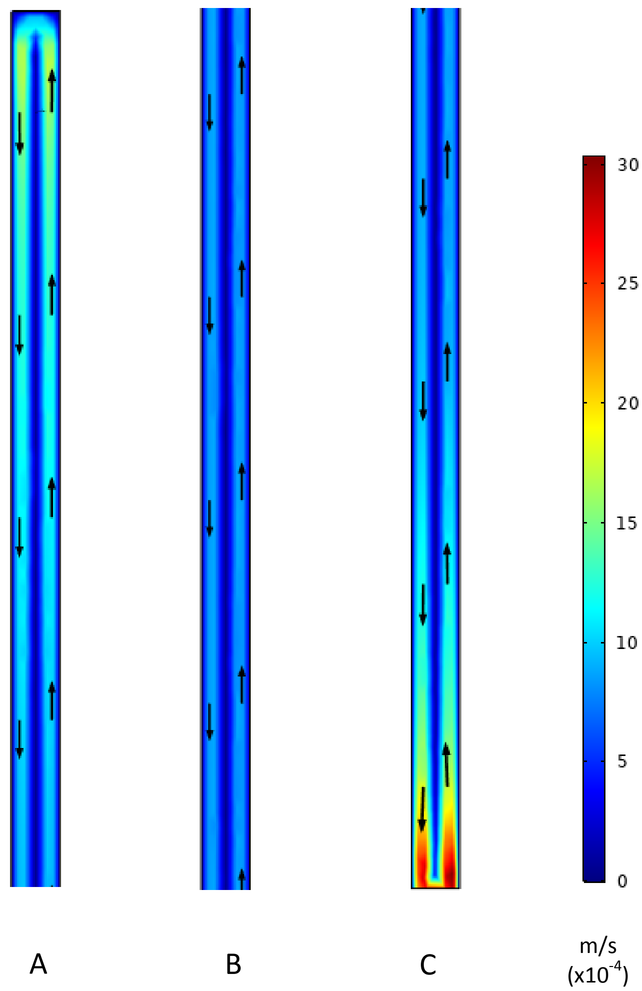

Temperature

Interior: 70°F (21.1°C)
Exterior: -10°F (-23.3°C)

Airflow Velocity

Average: 0.00058 m/s
Minimum: 0 m/s
Maximum: 0.003 m/s

6.4 Results: Three-Dimensional Analysis – Upper Wall Section

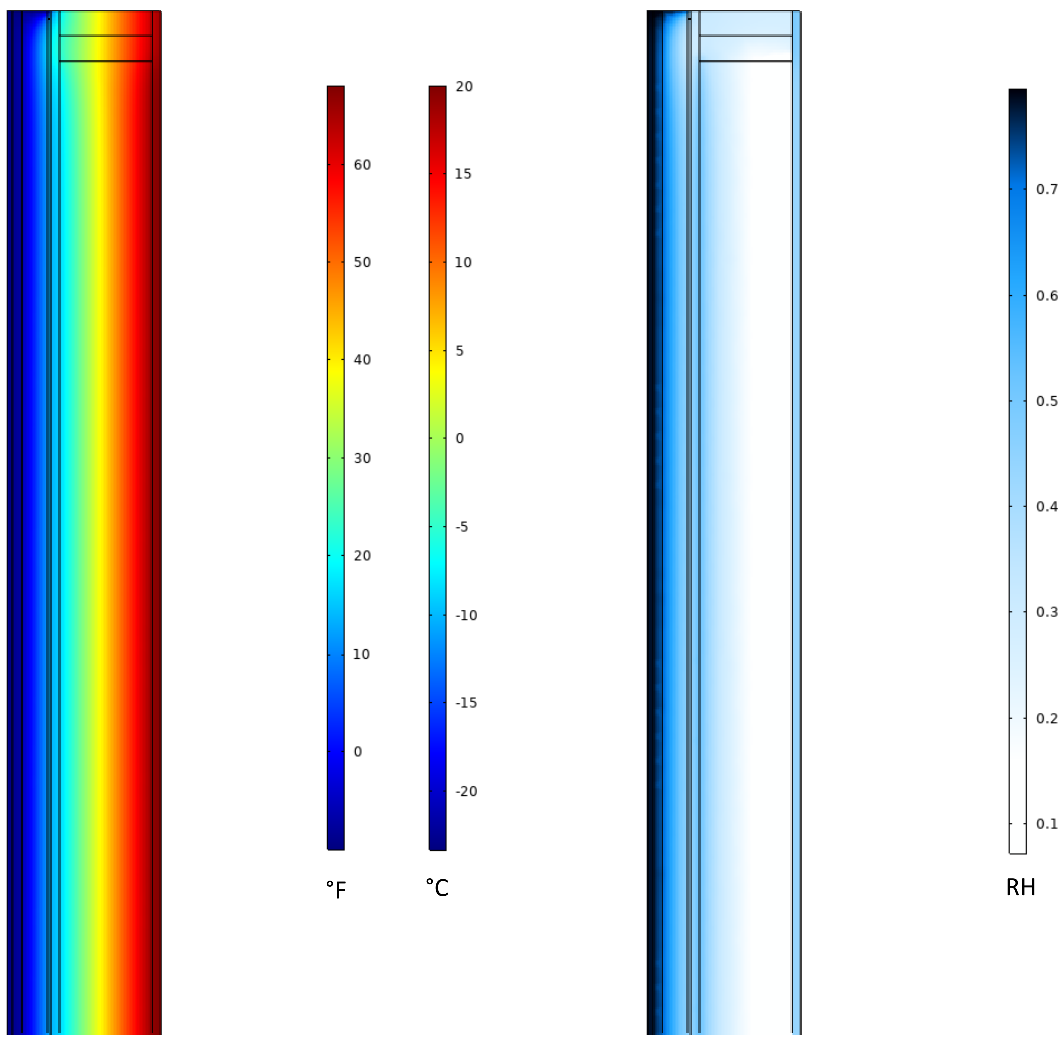

Temperature **Relative Humidity**

6.5 Results: Three-Dimensional Analysis – Lower Wall Section

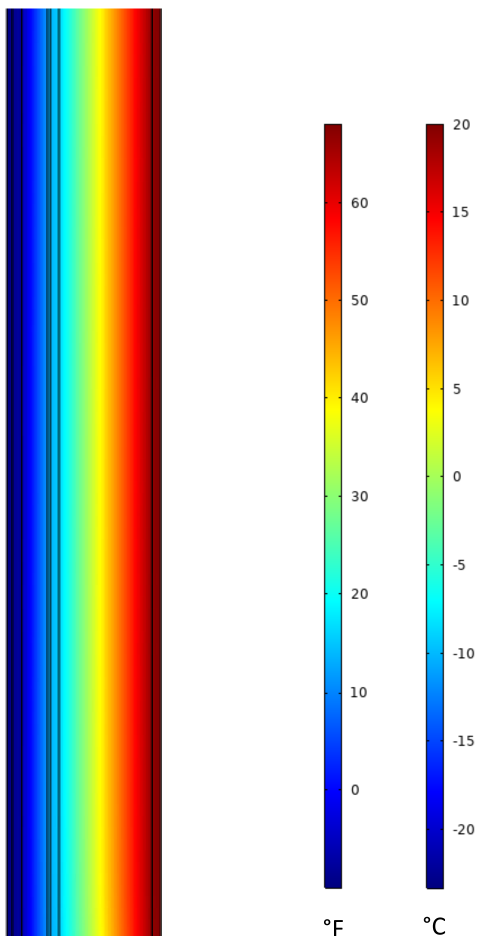

Temperature

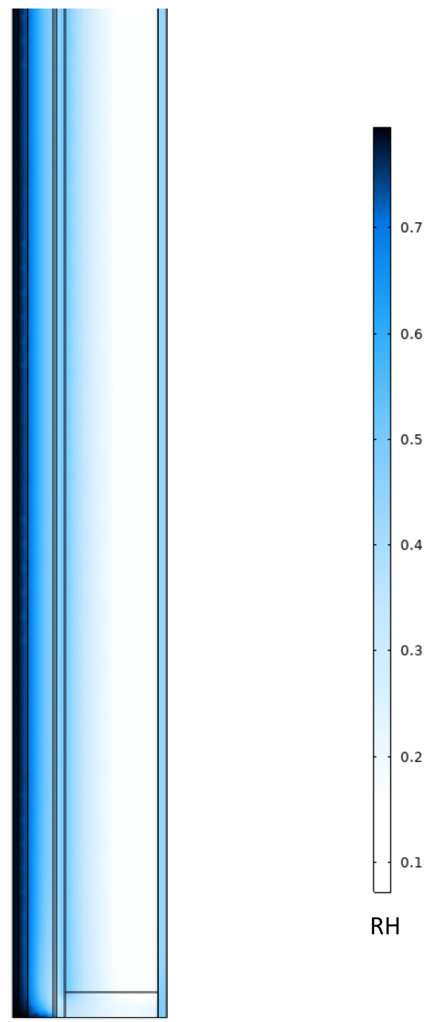

Relative Humidity

6.6 Results: Three-Dimensional Analysis – Plan View at Mid-Wall Height

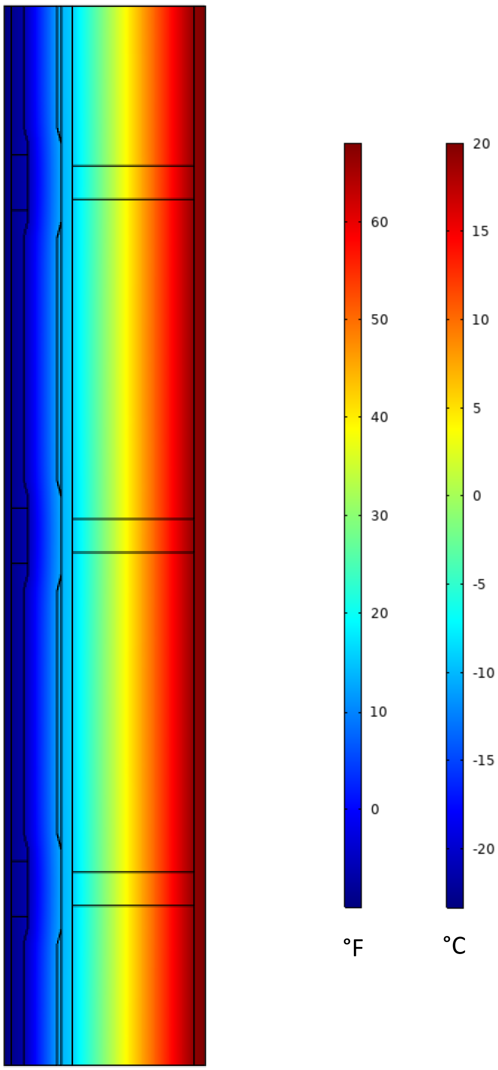

Temperature

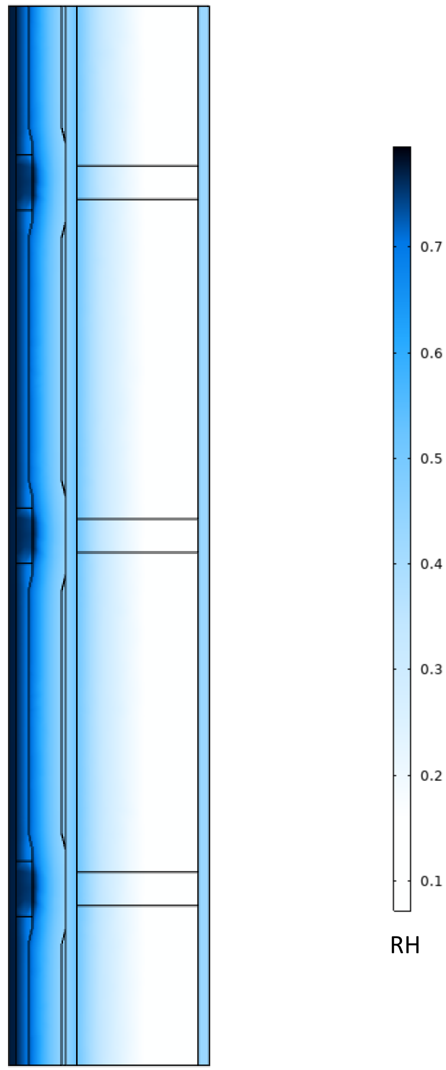

Relative Humidity